Dianthin-30 or gelonin versus monomethyl auristatin E, each configured with an anti-calcitonin receptor antibody, are differentially potent *in vitro* in high grade glioma cell lines derived from glioblastoma

Roger Gilabert-Oriol[1*], Sebastian G.B. Furness[2*], Brett W. Stringer[3], Alexander Weng[4,5], Hendrik Fuchs[4], Bryan W. Day[3], Angela Kourakis[1], Andrew W. Boyd[3], David L. Hare[1], Mayank Thakur[4], Terrance G. Johns[6], Peter J. Wookey[1].

[1]Department of Medicine (Austin Health, Heidelberg), University of Melbourne, Victoria, Australia

[2]Drug Discovery Biology Laboratory, Monash Institute of Pharmaceutical Sciences & Department of Pharmacology, Monash University (Parkville), Victoria, Australia

[3]QIMR-Berghofer Medical Research Institute, Brisbane, Queensland, Australia

[4]Institut für Laboratoriumsmedizin, Klinische Chemie und Pathobiochemie, Charité - Universitätsmedizin Berlin, Campus Virchow-Klinikum, Augustenburger Platz 1, 13353 Berlin, Germany.

[5]Institute of Pharmacy, Königin-Luise-Str. 2+4, 14195 Berlin, Germany.

[6]Hudson Institute of Medical Research, Monash University (Clayton), Victoria, Australia.

***** These authors contributed equally to this work

Roger Gilabert-Oriol's present address is: Department of Experimental Therapeutics, BC Cancer Research Centre, 675 W 10th Ave, Vancouver, BC, V5Z IL3, Canada.

Corresponding author

Dr Peter J Wookey,

University of Melbourne,

Department of Medicine/Cardiology

Lance Townsend Building, Level 10,

Austin Campus, Austin Health,

Studley Road,

Heidelberg, VIC 3084.

AUSTRALIA.

Email: pwookey@unimelb.edu.au

Abstract

We have reported that calcitonin receptor (CTR) is widely expressed in biopsies from the lethal brain tumour *glioblastoma* by malignant glioma and brain tumour initiating cells (glioma stem cells) using anti-human CTR antibodies. A monoclonal antibody against an epitope within the extracellular domain of CTR was raised (mAb2C4), and chemically conjugated to either plant ribosome-inactivating proteins (RIPs) dianthin-30 or gelonin, or the drug monomethyl auristatin E (MMAE), and purified. In the high grade glioma cell line (HGG, representing glioma stem cells) SB2b, in the presence of the triterpene glycoside SO1861, the EC_{50} for mAb2C4:dianthin was 10.0 pM and for mAb2C4:MMAE (antibody drug conjugate [ADC]) 2.5 nM, 250-fold less potent. With the cell line U87MG, in the presence of SO1861, the EC_{50} for mAb2C4:dianthin was 20 pM, mAb2C4:gelonin, 20 pM, compared to the ADC (6.3 nM), which is >300 less potent. Several other HGG cell lines that express CTR were tested and the efficacies of mAb2C4:RIP (dianthin or gelonin) were similar. Co-administration of the enhancer SO1861 purified from plants enhances lysosomal escape. Enhancement with SO1861 increased potency of the immunotoxin (>3 log values) compared to the ADC (1 log). The uptake of antibody was demonstrated with the fluorescent conjugate mAb2C4:AlexaFluor 568 and the release of dianthin-30:AlexaFluor488 into the cytosol following addition of SO1861 supports our model. These data demonstrate that the immunotoxins are highly potent and that CTR is an effective target expressed by a large proportion of HGG cell lines representative of glioma stem cells and isolated from individual patients.

Key Words: Calcitonin receptor; immunotoxins; targeting; high grade glioma cell lines; glioblastoma.

Précis

High grade glioma cell lines were exposed to immunotoxin (dianthin, gelonin conjugated to an anti-calcitonin receptor antibody) and were more potent (EC_{50} 10 pM) than the antibody:drug conjugate (MMAE) by 250-fold in the presence of enhancer SO1861.

Abbreviations

ADC	antibody-drug conjugate
BTIC	brain tumour initiating cell
CTR	calcitonin receptor
DTT	dithiothreitol
EDTA	ethylene diamine tetra acetate
EGF	epidermal growth factor
EGFR	epidermal growth factor receptor
FGF	fibroblast growth factor
GBM	glioblastoma multiforme
hCTR	human calcitonin receptor
HGG	high grade glioma
LDH	lactate dehydrogenase
MMAE	monomethyl auristatin E
NTA	nitrilotriacetate
RIP	ribosome-inactivating protein
VEGF	vascular endothelial growth factor.

Introduction

Successful treatment of recalcitrant tumours remains one of the great challenges of cancer research. One such recalcitrant tumour, *glioblastoma* (GBM), is a deadly brain tumour (grade 4 astrocytoma [1]). One of the underlying features of GBM is the invasive potential of brain tumour initiating cells (BTIC) [2] which are regarded as clones of cells with stem-like properties (glioma stem cells) [3, 4]. These cells are considered to have the capacity to differentiate into a variety of cell types [5] including endothelial cells and pericytes, which are essential for the maintenance and expansion of the solid tumour. Thus it is considered that these stem-like cells provide the malignant basis of glioblastoma and hence represent potentially important targets for treatment.

Conventional chemo- and radio-therapies, cyto-reductive surgery and trialled treatment modalities including Avastin (anti-VEGF antibody) therapy, have had minimal impact on the mean survival after diagnosis, which remains low at just 14-17 months [6].

The deployment of antibody drug conjugates (ADC) to treat recalcitrant tumours is a relatively recent research strategy in which the number of lead ADCs entering clinical trials has increased rapidly [7-9]. Successful treatment is partly dependent on the properties of the antibody and its target, for efficient delivery of the drug into the tumour cell, as well as the efficacy of the drug itself. Recently, an ADC based on an anti-EGFRvIII antibody (ABT-806) conjugated to monomethyl auristatin F (MMAF) resulting in an ADC (ABT-414) has been demonstrated to be effective in 22% of GBM patients in a phase I study [10].

Immunotoxins made from antibodies conjugated with either bacterial or plant toxins have been investigated for many years and there are examples of the former that have reached clinical trials. However, studies involving plant-based immunotoxins have been less frequent and the development of ADCs for clinical trials is more advanced. However, recent advances in immunotoxin research are beginning to change this preference. Firstly, plant toxins such as the ribosome-inactivating proteins (RIP) dianthin-30 [11] and gelonin

[12] (originally extracted from seeds) are now synthesised as functional recombinant proteins. Secondly, when administered in combination with enhancers of lysosomal escape (non-toxic co-factors) such as the triterpene glycoside SO1861 [13] there is a decrease by several orders of magnitude in the effective concentration (EC_{50}) for cytotoxicity. This enhancer is a plant triterpene glycoside, purified from the plant *Saponaria officinalis* L. [13], with specific structural features that enhance the cytotoxicity of immunotoxins conjugated with RIPs. SO1861 has a triterpenoidal skeleton of oleanane type and two sugar side chains (bisdesmosidic) attached to it at positions C-3 and C-28 [14]. Such enhancers interact at non-toxic concentrations with the immunotoxin within the endosomal or lysosomal compartment of the target cells [14] and promote release into the cytosol [15] where the toxin targets ribosomes.

Our understanding of the role of calcitonin receptor (CTR) in cell physiology has been evolving over the last 20 years with new knowledge of the mechanisms of agonist bias [16] and an increasing appreciation of the broad range of tissues in specific physiological states, in which CTR is expressed. For instance, CTR expression may be transitory in wound healing [17] and in neurons of the gut around birth [18]. It is expressed by activated lymphocytes [19, 20] and during foetal development [21-23]. Recently, we have proposed that CTR is externalised during the pre-apoptotic cell stress response [24].

CTR is a target of interest because it is expressed by malignant tumor cells of the brain tumor *glioblastoma* [25]. Furthermore, CTR is also expressed in other malignancies including multiple myeloma [26], leukemia [17], lymphoma [27], bone tumors [28, 29], breast [30] and prostate cancers [31, 32], and medullary thyroid cancers [33]. The function(s) of CTR in the contexts of these different cancers is largely unknown, however an anti-apoptotic or survival activity has been proposed together with metabolic reprogramming [27].

Important considerations in the design of immunotoxins for the treatment of cancers includes the sufficient expression of the target receptor on the surface of BTICs compared to other exposed tissues [34] and internalisation of receptors with the immunotoxin attached. High grade glioma (HGG) cell lines [35] derived from GBM, represent BTICs and include the subtypes, pro-neural, neural, classical and mesenchymal, classified according to gene profiling. Five HGG cell lines (BAH1, JK2, PB1, SB2b & WK1 [36]) out of the twelve originally tested (~40%) were shown to express human CTR (hCTR) on immunoblots and four of these plus two others from a separate source, were included in this study. CTR-positive HGG cell lines represent each of the subtypes listed above. These HGG cell lines, when injected intracranially into immuno-deficient mice, form GBM-like tumours [37].

In this study CTR is evaluated as a potential target expressed by HGG cell lines and as an uptake mechanism for internalisation of immunotoxins. For comparison, the efficacies of two anti-CTR immunotoxins based on an anti-CTR antibody conjugated to the plant toxins dianthin-30 and gelonin, and an ADC with monomethyl auristatin E [38], are reported here with and without SO1861. Monomethyl auristatin is included in this study as it is frequently incorporated into ADCs tested in clinical trials and reported in the literature [7-9] due to its toxicity as an anti-microtubule agent.

Materials and Methods

High Grade Glioma cell lines

In total seven HGG cell lines out of 14 screened expressed detectible levels of calcitonin receptor as determined by immunoblot. These include four (JK2 [39], PB1 [40], SB2b [41] & WK1 [36, 41]) from the QIMR-Berghofer Medical Research Institute (Brisbane, Australia). Two further cell lines GBM-4 and GBM-L2 [42] were obtained from the Monash Institute of Medical Research (Professor TG Johns). These lines were all grown on Matrigel (Corning, US)-coated plastic surfaces under serum-free conditions in StemPro® NSC SFM - Serum-Free Human Neural Stem Cell Culture Medium (Thermo Fisher Scientific, US) with EGF, FGF2, glutaMAX plus penicillin/streptomycin (Thermo Fisher Scientific) and cultured at 37°C in a 95% humidified air, 5% CO_2 atmosphere [37].

The cell line U87MG, described extensively in the literature and derived from glioblastoma, was also included to provide a reference point for other published studies. U87MG was maintained in DMEM-F12/10% FBS plus penicillin/streptomycin (Thermo Fisher Scientific) grown at 37°C in an atmosphere of 5% CO_2. For efficacy studies in the 96-well format and growth in chamber slides for confocal analysis, U87MG cells were cultured on Matrigel under identical serum-free conditions used for HGG cell lines, in StemPro® NSC SFM.

Ribosome-inactivating proteins (RIP) and the drug monomethyl auristatin E (MMAE)

The RIP dianthin-30 [His^6] was synthesised as a recombinant protein in *E. coli* and purified by affinity (nickel-nitrilotriacetic acid [NTA] agarose) chromatography [43]. rGelonin was a gift from Professor Michael G Rosenblum (MD Anderson Cancer Center, Texas) which was synthesised and purified from *E. coli* [44]. MMAE (OSu-Glu-VC-PAB-MMAE) was purchased from Concortis Biosystems Corp., (US).

178 **The enhancer triterpene glycoside SO1861**

179 The extraction and isolation of the enhancer SO1861 from plant roots of *Saponaria*
180 *officinalis* L. Caryophyllacea has been described [13]. The chemical structure of SO1861
181 has been solved and will be published in detail elsewhere (Dr Alexander Weng, personal
182 communication). At 3 µg/mL used in the growth assays, SO1861 is slightly toxic resulting
183 in 10% retardation of cell proliferation. For U87MG cells the concentration used was 1
184 µg/mL.

185

186 **Antibodies**

187 These studies involved the use of a mouse monoclonal anti-human CTR antibody
188 (mAb 46/08-2C4-2-2-4 [IgG1]) directed against an extracellular epitope (Welcome
189 Receptor Antibodies [WRA, Melbourne) [24]. MAb1H10 (IgG_{2A}) was raised against a
190 cytoplasmic epitope (mAb 31/01-1H10, WRA, Melbourne; also distributed as MCA 2191 by
191 BioRad, UK). These antibodies have been previously validated (in the supplementary
192 materials linked to [24]) and further data published elsewhere [25].

193

194 **Conjugation of toxins to mAb2C4**

195 Dianthin-30[His^6] or gelonin was conjugated to mAb2C4 using succinimidyl 3-(2-
196 pyridyldithio) propionate (SPDP, Thermo Fisher Scientific). This cross-linking procedure
197 introduced a covalent disulphide bridge between the toxins and the monoclonal antibody.
198 In the case of dianthin-30[His^6] and mAb2C4, both proteins (molar ratio 1:1) were modified
199 by SPDP and the molar ratios that were considered for their chemical reaction were
200 protein:cross-linker of 1:3, 1:6 and 1:12. In the case of gelonin and mAb2C4, in a first
201 attempt both proteins (molar ratio 1:1) were modified by SPDP at a molar ratio
202 protein:cross-linker of 1:6. In a second and third attempt, only mAb2C4 (molar ratio

gelonin:mAb2C4 of 3:1) was modified by SPDP at a molar ratio of protein:cross-linker of 1:3 and 1:6.

In brief, proteins (dianthin-30[His^6], gelonin and mAb2C4) were equilibrated in PBS-EDTA buffer (20 mM sodium phosphate, 150 mM sodium chloride, 1 mM EDTA, 0.02% sodium azide, pH 7.5) using a 5 mL Zeba polyacrylamide de-salting columns (Thermo Fisher Scientific). Proteins were modified by addition of SPDP (20 mM in DMSO) for 60 min at room temperature. Proteins were desalted again using 5 mL Zeba de-salting columns and then SPDP-modified toxin was reduced with the addition of dithiothreitol (DTT, final concentration of 50 mM) for 30 min at room temperature. DTT was removed using a Zeba de-salting column. Monoclonal antibody and reduced toxins (or non-modified gelonin containing one available cysteine) were allowed to react for 18 h at room temperature. The conjugates were stored at 4°C pending further purification.

Monomethyl auristatin E (MMAE) was conjugated to mAb2C4 via the cross-linker OSu-Glu-VC-PAB as indicated by the manufacturer (Concortis Biosystems Corp, US). The chemical reaction was performed with a molar ratio mAb2C4:OSu-Glu-VC-PAB-MMAE of 1:7. The antibody was equilibrated in the conjugation buffer 1 (CB1, 50 mM potassium phosphate, 50 mM sodium chloride, 2 mM EDTA, pH 6.5) using a 5 mL Zeba de-salting column. Antibody was modified by addition of OSu-Glu-VC-PAB-MMAE (10mM in DMA). Further organic solvent was added up to 10% (v/v) DMA and cross-linking reaction run for 18 h at room temperature. The reaction was stopped by exchanging the CB1 with the conjugation buffer 2 (CB2, 50 mM sodium succinate, pH 5.0) using a 5 mL Zeba de-salting column. Antibody-drug conjugate was stored at 4°C pending further purification steps.

Purification of immunotoxins and the ADC

MAb2C4:dianthin-30[His^6]. The first step in purification involved chromatography with a nickel-NTA agarose matrix (Life Technologies).

In brief, 20 mM imidazole in buffer (50 mM sodium phosphate, 300 mM sodium chloride [pH 8.0]) was added to the crude cross-linked reaction mix, mixed with nickel-NTA agarose (3 mL bed volume) and equilibrated with inversion at 25°C for 60 min. The bound matrix was poured into a 10 mL column, with gravity feed and washed with 3 column volumes of binding buffer (as above). The bound products were eluted with 250 mM imidazole in buffer. The eluted proteins (mAb2C4:dianthin-30[His^6] and dianthin-30[His^6]) were dialysed against PBS overnight at 6°C.

The second step of purification was achieved with chromatography on a peptide affinity column (thiopropyl sepharose 6B, prepared by Mimotopes, Clayton, Australia) using the peptide sequence (CSGS-PSEKVTKYCDEKGVWFK, synthesised by Mimotopes) equivalent to the extracellular epitope of human CTR that binds mAb2C4. This step excluded antibody products in which the binding determinants for the peptide sequence had been compromised during the conjugation step. The dialysed material was passed down the affinity column, washed in 3 volumes of 20mM sodium phosphate (pH 7.0), eluted with 100 mM glycine (pH 2.2) and the fractions neutralised with 10% of the collected volume with 1 M TRIS (pH 9.0). These fractions were dialysed overnight in PBS and concentrated using Amicon Ultra-15 centrifugal filters (10 kD cut off). The yield of conjugated material after purification was approximately 8%, compared to the initial amounts of dianthin-30[His^6] and mAb2C4 used in the conjugation.

MAb2C4:gelonin The conjugated crude product mAb2C4:gelonin was purified in a two-step process, firstly with the affinity column described above. The second chromatographic step was dependent on the binding of the product to HiTrap Blue HP matrix (GE Healthcare) [44, 45] and elution with sodium chloride. The yield of the final product (mAb2C4:gelonin) was similar to that of mAb2C4:dianthin-30[His^6].

MAb2C4:MMAE The conjugated crude solution of mAb2C4:MMAE was also purified by two chromatographic steps, firstly with the peptide affinity column described above. This

purification step eliminates inactive binding products of mAb2C4:MMAE that might have been generated during the conjugation as they pass through within the void volume. The second step in purification was chromatography on a hydrophobic interactive matrix (HiTrap Phenyl HP, GE Healthcare) and the active fraction was eluted with a reverse ammonium chloride gradient.

Growth/cytotoxicity assays in the 96-well format

For efficacy studies in the 96-well format all cell lines were grown on Matrigel (Corning, US) under serum-free conditions in StemPro® NSC SFM (Life Technologies/Thermo Fisher Scientific) with growth factors and seeded at 2,500 cells per well. Two to three hours after plating the cells, additions such as SO1861 and immunotoxins (mAb 2C4:dianthin-30[His^6], mAb2C4:gelonin) or ADC (mAb2C4:MMAE) were made. Control plates included mAb2C4 with SO1861 or immunotoxin without SO1861. Cells were incubated at 37°C for 4 days (U87MG) or 6 days (HGG cell lines). Total lactate dehydrogenase (LDH, lysed cells) and residual LDH (non-lysed samples) were performed in triplicate. LDH measured using an LDH cytotoxicity detection kit (Roche) and read on a FLUOstar OPTIMA (BMG Labtech).

Confocal microscopy of HGG cell lines and immuno-fluorescence with multi-channel detection

The confocal analysis of the uptake of mAb2C4 into HGG cell lines was accomplished with mAb2C4 labelled with AlexaFluor 568 (AF568, Thermo Fisher Scientific) using conjugation of lysines with NHS succinimidyl esters of AF568 [24].

HGG cell lines were cultured (described above) to 50-80% confluence on 4-well glass slides (Lab Tek II chamber slides, NUNC) coated with Matrigel (Corning, US) in a humidified incubator (5% CO_2) at 37°C then washed with media without growth factors.

MAb2C4:AF568 (1 µg/mL) was added to 1 mL of fresh growth medium and the chamber slides incubated for 24 h in the incubator.

Cells were washed with PBS, fixed with 4% paraformaldehyde/PBS for 30 min and then washed twice with PBS. Cells were blocked with 5% normal goat serum/1% bovine serum albumin for 1 h.

Slides of fixed cells were incubated overnight at 6°C with rabbit anti-LAMP1 antibody (Cell Signalling) that detects lysosomes. The secondary antibody used was goat anti-rabbit AlexaFluor 488 (4µg/mL, Thermo Fisher Scientific). The samples were then mounted using DAPI aqueous mount (Prolong Gold, Thermo Fisher Scientific) to visualise the nuclei and dried at RT for several days in the dark. The samples were imaged by confocal microscopy (Objectives x20 and x63) on a Zeiss Imager Z1/LSM 510 Meta confocal laser scanning system using Zen software. Images (LSM format) were captured in a single focal plane (optical sections of 0.7 µm nominal thickness) or using the Z-series feature where ~ 15 optical sections were compressed (devolution using LSM Image Browser, Zeiss) to create a single plane image (TIFF format) equivalent to approximately 10 µm tissue thickness.

Live cell imaging

U-87 MG (ATCC® HTB-14™) cells were seeded (2000/dish) in Ibidi µ-Dishes (35 mm, low, Martinsried, Germany) and cultured in 2 mL Dulbecco's MEM supplemented with 10% fetal bovine serum and 1% penicillin/streptomycin. After 92 h, the medium was removed and 1 mL fresh culture medium was added. Dianthin:AF488 (100nM) was added and cells were incubated over night for an incubation period of 18 h. Dianthin was labelled beforehand with Alexa-Fluor 488 5-TFP ester (Life Technologies) as described previously [46].

306 The live cell imaging marker pHrodo™ Red Dextran (final concentration 40 µg/ mL,
307 Life Technologies) was added 6 h before the end of the incubation period. pHrodo™ Red
308 Dextran is a live cell imaging marker for acidic intracellular compartments such as
309 lysosomes. Hoechst 33342 (Life Technologies) was added 30 min before the end of the
310 incubation period. Cells were washed with PBS (3×), covered with 1 mL live cell imaging
311 solution (Life Technologies), supplemented with 1% FBS and 20 mM D-glucose and
312 analyzed using a LSM780 laser scanning microscope, Axio Observer Z1 with a Plan-
313 Apochromat 63×/1.4 Oil Objective (Carl Zeiss, Jena, Germany). Cells were maintained at
314 37°C throughout the experiment. Cells were continuously monitored (supplementary video)
315 and 36 s after the start of the analyses SO1861 was added at a final concentration of 5
316 µg/mL. To determine the SO1861 induced endosomal escape of dianthin:AF488 into the
317 cytosol, regions of interest were assigned for individual cells and the increase of intensity
318 was determined offline using ZEN 2.3 lite software (Carl Zeiss).
319

Results

The principal aim of this study was to synthesize conjugates of mAb2C4 antibody including the immunotoxins mAb2C4:dianthin-30, mAb2C4:gelonin and the antibody:drug conjugate (ADC) mAb2C4:MMAE, for comparison of their efficacies to promote cell death in high grade glioma cell lines and U87MG. The validation of mAb2C4, which binds to an extracellular linear epitope (epitope 4) of human CTR, has been presented elsewhere [24].

Expression of calcitonin receptor protein was determined by immunoblot

In Fig. 1a is shown expression of CTR protein by HGG cell lines and the cell line U87MG, probed with the antibody mAb1H10 which recognises an intracellular epitope (band 'a'). In U87MG cells probed with mAb2C4 (band 'b') is shown the target of MW~55 kD. Band 'c' is a product of degradation of CTR.

Syntheses and purification steps for immunotoxins and ADC

Chromatography with the peptide affinity column constructed with the peptide sequence used for immunization and the cloning/expression of mAb2C4, was used for purification of each conjugate (immunotoxin or ADC), and mAb2C4:AF568 (see Fig. 3) as the bound material retains the capacity to bind to epitope 4 of CTR. Any antibody with compromised binding capacity passes through in the flowthrough during chromatography.

In Fig. 1 b-e are images of SDS-PAGE gels which represent the stages of synthesis (Fig. 1b, crude product, lane 1 and lane 2 [reduced] compared to mAb2C4 alone) and the purified mAb2C4:dianthin-30[His^6] (Fig. 1c), following chromatography on nickel-NTA column and the peptide affinity column. In Fig. 1d is shown the profile of purified mAb2C4:gelonin following chromatography on the peptide affinity and HiTrap Blue HP columns, and in Fig. 1e, purified mAb2C4:MMAE following chromatography on a peptide affinity column and HiTrap Phenyl HP. Further details of the purifications of

mAb2C4:dianthin, mAb2C4:gelonin and mAb2C4:MMAE can be found supplementary figures 1-3.

The comparative potency of immunotoxin versus ADC in HGG cell line SB2b and cell line U87MG

In Fig. 2a, using the HGG cell line SB2b, are the graphical displays from the results of multiple experiments with mAb2C4:dianthin (n=4) with and without SO1861, compared to mAb2C4:MMAE (n=4) [Fig. 2b with and without SO1861]. With SO1861 the negative logarithm of the half maximal effective concentration (pEC_{50}) for mAb2C4:dianthin was calculated, using a 3 parameter logistic equation, as -11.0 ± 0.14 (EC_{50}, 10.0 pM) and for mAb2C4:MMAE as -8.6 ± 0.20 (EC_{50}, 2.5 nM) which is approximately 250-fold less potent (Table 1).

In the HGG cell line SB2b, SO1861 increased the potency of mAb2C4:dianthin-30 by 3 log values (from supplementary figure 7) and mAb2C4:MMAE by 1 log value (Fig. 2b). With the HGG cell line JK2 treated with mAb2C4:dianthin and SO1861 (supplementary figure 5) the EC_{50} was 10.0 pM (Table 1), similar to the value calculated for SB2b.

We tested the biological activity of mAb2C4:dianthin-30 and mAb2C4:MMAE in the cell line U87MG as a reference cell line for comparison with other studies reported in the literature. In the presence of SO1861 (Fig. 2c) the EC_{50} was 20.0 pM and 6.3 nM (Table 1) respectively, which is 300-fold less potent. The EC_{50} for mAb2C4:gelonin was similar to that for mAb2C4:dianthin-30, namely 20 pM (Table 1).

The potency of each immunotoxin vs ADC in a range of GBM cell lines

The EC_{50} values in several high grade glioma cell lines are listed in supplementary table 1 after one experimental determination. The values for mAb2C4:dianthin-30 in the

presence of SO1861 are close to 10 pM for SB2b, JK2, GBM-4 and GBM-L2, approximately 50 pM for WK1, but PB1 is quite resistant to both mAb2C4:dianthin-30 and mAb2C4:gelonin (supplementary figures 6, 7 and supplementary table 1).

The uptake of mAb2C4:AF568 into HGG cell lines and U87MG

In Fig. 3 is shown images of the uptake of mAb2C4:AF568 by cell lines JK2 (low [x20] magnification), and at higher [x63] magnification, SB2b, PB1 and U87MG. Fluorescence associated with mAb2C4:AF568 is present on the cell membranes as well as concentrated in the perinuclear region. Some of the latter fluorescence coincides with LAMP1 staining (green in Fig. 3 d and f) as shown in yellow [overlap], although the extent of LAMP1-positivity varies considerably between the cell lines. LAMP1 is commonly used to identify the late endosomal/lysosomal compartments.

Of note PB1, which is relatively resistant to mAb2C4:dianthin-30 showed uptake of mAb2C4:AF568 following live staining for one hour.

Triterpene glycoside SO1861 promotes the release of dianthin into the cytosol

The release of toxin with enhancer SO1861 from intracellular compartments was tested by pre-loading the U87MG cells with Alexa Fluor 488-labelled dianthin (dianthin:AF488) prior to real time imaging. In Fig. 4 a-d, U87MG cells were incubated with the nuclear stain Hoechst 33342 (Fig. 4a), pHrodo™ Red Dextran (Fig. 4b), which is a marker for endosomes and lysosomes, and dianthin:AF488 (Fig. 4c; merged image Fig. 4d). Dianthin:AF488 was detected in intracellular vesicles (Fig. 4c) and co-localisation with pHrodo™ Red Dextran was observed (white arrows), indicating that dianthin:AF488 was transported into endosomes/lysosomes.

In further real time experiments, SO1861 was added to the cells in order to investigate the SO1861 mediated intracellular release of dianthin:AF488 into the cytosol.

This is quantified in Fig. 4e. The complete video sequence can be found in the supplementary video. The cytosolic fluorescence indicates the release of dianthin:AF488 from intracellular compartments, a process that is mediated by SO1861. In Fig. 4 (f-i) are shown images taken from the supplementary video 1: panel (f) at 36 s when 5 µg/mL SO1861 was added, panel (g) at 136 s (no change), panel (h) at 180 s when dainthin:AF488 was released into the cytosol of cell 1 and panel (i) at 500 s when dainthin:AF488 was released into the cytosol of cell 2.

Discussion

CTR was found expressed in a high percentage of human biopsies of glioblastoma [25] and as reported here, by approximately 50% of HGG cell lines that were available to us. These cell lines are considered to represent glioma stem cells. In view of their role in the rapid expansion of the tumour and the relative resistance glioma stem cells confer to conventional therapies, we chose to target CTR and compare the efficacies of antibody:conjugates representing two immunotoxins and an ADC. Part of the reasoning was the current popularity of ADCs being tested in clinical trials and our own interest in the potency of enhancers to improve the efficacy of RIP-based immunotoxins. Thus the question we addressed concerned the comparison of the efficacies of immunotoxins and a related ADC tested on HGG cell lines *in vitro*.

The opportunity for this study began with our identification of the expression of CTR in glioblastoma and the validation of the antibody mAb2C4 which specifically binds an extracellular epitope of hCTR [24].

The first step was the synthesis of immunotoxins from mAb2C4 and the RIPs, diathin-30 [43] and gelonin [44], and the drug MMAE [38] with a linker, together known as vedotin. A range of protein (antibody or toxin) and cross-linker SPDP molar ratios were tested and the optimal 1:6 for both were conjugated and further purified as described. One important step in purification for each synthesis employed chromatography using a peptide affinity column which selected moieties that were capable of specifically binding the target sequence of hCTR located in the extracellular N-terminal domain and excluded modified antibody conjugates that no longer retained affinity for CTR.

Following the purification steps we determined with statistical accuracy the efficacy of treatment with mAb2C4:dianthin compared to mAb2C4:MMAE which involved 96-well assays to determine nett LDH and these were repeated four times (data shown in Fig. 2a - c). With the HGG cell line SB2b, in the presence of SO1861, the EC_{50} for

mAb2C4:dianthin is 10.0 pM and for mAb2C4:MMAE 2.5 nM, which is approximately 250-fold less potent. Similarly with the cell line U87MG, in the presence of SO1861, the EC_{50} for mAb2C4:dianthin is 20.0 pM and for mAb2C4:MMAE 6.3 nM, which is approximately 300-fold less potent.

To further explore the underlying biological variation that might be expected between patients we pooled the data for all HGG cell lines tested (data not shown) and U87MG treated with either mAb2C4:dianthin or mAb2C4:gelonin (EC_{50} for both, 8 pM), but excluded the data derived with the HGG cell line PB1, which was resistant to both the immunotoxins. A comparison with the pooled for the ADC (EC_{50}, 10 nM) demonstrated the immunotoxins were greater than 3 logs more potent. These pooled data demonstrate a remarkably similar sensitivity to both immunotoxins in a range of HGG cell lines. This observation adds weight to the claim that CTR is a potential target for the treatment of glioblastoma as a high proportion of lines that express CTR were sensitive to the immunotoxins and were isolated from individual biopsies.

MAb2C4:MMAE was consistently less potent, with EC_{50} in the nM range for both SB2b and U87MG, which is 250-300 times less potent than mAb2C4:dianthin-30 and mAb2C4:gelonin in the presence of SO1861. Controls with unconjugated antibody (in the higher nM range) showed little effect on cell death. In the absence of SO1861 mAb2C4:MMAE is 10 fold less potent and mAb2C4:RIPs were relatively ineffective (1000 fold less potent) such that their potencies are similar at approximately 10-20 nM (Table 1 and supplementary figure 6). These data demonstrate the enhancer SO1861 has a high degree of specificity for the RIP. The EC_{50} data for these cell lines with mAb2C4:RIPs as described above is consistent with data published recently for cetuximab:dianthin-30 (5.3 pM), panitumumab:dianthin-30 (1.5 pM) and trastuzumab:diathin-30 (23 pM) co-administered with SO1861 [43].

The HGG cell line PB1 was resistant to mAb2C4:RIPs although it expressed CTR as determined by immunoblot (Fig. 1a) and accumulated mAb2C4:AF568 (Fig. 3). This demonstration of resistance by PB1 alone compared to other cell lines, supports a mechanism in which uptake of immunotoxin is receptor-mediated rather than some non-specific mechanism of internalisation. Possible explanations for resistance in this cell line include that CTR is not efficiently internalised to reach the lysosomal compartment or the immunotoxin is not cleaved in the lysosomal compartment or that the RIP is not released into the cytosol. We note the significant difference in the intracellular distribution of mAb2C4:AF568 in PB1 compared with SB2b and U87MG. The large concentration of antibody suggests stalling and localisation in a peri-nuclear structure, perhaps the microtubule organising centre, with little access to the lysosomal compartment.

Seck et al [47] originally proposed that CTR is embedded in the endosomal membrane and that this structure is bound to the cytoskeleton through the intermediate filament filamin. We have extended this idea [24] in which carboxyl terminal arginines together with a PDZ docking site are identified in all species and are predicted to be important sites of binding to tubulin. We proposed that the mechanism of uptake of mAb2C4 conjugates was driven by receptor-mediated endocytosis with endosomes trafficked along the microtubules driven by molecular motors as reviewed [48]. When immunotoxins are transported by these endosomes, which subsequently become transformed into lysosomes (at low pH), the enhancers induce the release of cleaved RIPs as illustrated in Fig. 4 and supplementary video 1. During this release, the RIP does not breach the plasma membrane in significant amounts but remains concentrated within the cytosol, consistent with the actions of enhancers in the release of RIP into the cytosol.

The relatively recent description of the powerful additional effects of enhancers and prior inefficient escape of RIPs from intracellular compartments in their absence, might be

a major reason why plant immunotoxins have not yet achieved acceptance for clinical studies. With successful animal studies this situation is likely to change.

Recent unpublished studies in mice by our group have investigated the toxicity of mAb2C4:dianthin with SO1861. The mice tolerate the highest serum concentration tested, namely 300 pM immunotoxin, with no apparent effects on health (unpublished results). Given the EC_{50} *in vitro* is approximately 10 pM this provides a potential therapeutic window. From these observations of tolerance it seems that CTR-neural circuits, the expression in distal tubules, thyroid and elsewhere, may escape exposure to the immunotoxin. Any depleted populations, perhaps osteoclasts, might be replenished from bone marrow progenitors. These results are also consistent with the lack of significant penetration of the vasculature in which endothelial cells are CTR-negative and supports the view that uptake of this immunotoxin into cells is a receptor-mediated process.

As far as we are aware this is the first published study in which an anti-G protein-coupled receptor antibody has been employed to target cancer stem cells. In view of the expression of CTR by a range of tumour types it seems likely that this technology could be included in strategies for the treatment of other cancers (or subtypes) including breast, bone, prostate cancers and others (see Introduction). We ask the question, is there a link between expression of CTR in cancer stem cells and expression in the pre-apoptotic cell stress response as proposed elsewhere [24]? In other words do some cancer cells exist in a state equivalent to the pre-apoptotic cell stress response?

In clinical trials immunogenicity associated with RIPs has been overcome with T-cell epitope depletion, for instance in the case of de-bouganin [49]. When combined with improved potency afforded with triterpene glycosides this is likely to create a powerful and effective combinational therapy for recalcitrant tumours.

In summary we have demonstrated that an anti-CTR antibody conjugated to an RIP can be deployed to target glioma stem cells (HGG cell lines). These cells form the basis

for resistance to chemotherapy and expansion of the deadly tumour glioblastoma. The immunotoxins studied here are 250-300 times more potent than an equivalent ADC in a range of HGG cell lines and suggests more potent, aggressive treatment regimens can be configured than are currently being investigated in clinical trials. This improved efficacy may be important for the successful treatment of recalcitrant tumours such as GBM and such strategies should be investigated with clinical trials as the next step to improve patient outcomes.

Acknowledgements

Dr Furness was supported by the National Health and Medical Research Council of Australia (Program Grant 1055134 and Project Grant 1061044). Dr Gilabert-Oriol was supported by an Endeavour Research Fellowship (Australian Government). This research did not receive any specific grant from funding agencies in the public, commercial, or not-for-profit sectors. The authors are grateful for the gift of rGelonin from Professor Rosenblum of the University of Texas MD Anderson Cancer Center, Texas, USA. Confocal Microscopy was performed at the Biological Optical Microscopy Platform, The University of Melbourne (www.microscopy.unimelb.edu.au) and *the Leibniz-Institut für Molekulare Pharmakologie* (FMP), Campus Berlin-Buch, Berlin, Germany. Thanks go to the team at the Antibody Facility (Walter & Eliza Hall Institute, Bundoora) for production of the anti-CTR antibodies.

Conflict of Interest

Dr Wookey is a Director of Welcome Receptor Antibodies Pty Ltd (Australia) which developed the anti-CTR antibodies. All other authors declare no conflict of interest.

References

1. Louis DN, Ohgaki H, Wiestler OD, Cavenee WK, Burger PC, Jouvet A, Scheithauer BW, Kleihues P (2007) The 2007 WHO classification of tumours of the central nervous system. Acta Neuropathol 114:97-109.
2. Galli R, Binda E, Orfanelli U, Cipelletti B, Gritti A, De Vitis S, Fiocco R, Foroni C, Dimeco F, Vescovi A (2004) Isolation and characterization of tumorigenic, stem-like neural precursors from human glioblastoma. Cancer Res 64:7011-21.
3. Reya T, Morrison SJ, Clarke MF, Weissman IL (2001) Stem cells, cancer, and cancer stem cells. Nature 414:105-11.
4. Fomchenko EI, Holland EC (2005) Stem cells and brain cancer. Exp Cell Res 306:323-329.
5. Das S, Marsden PA (2013) Angiogenesis in glioblastoma. N Engl J Med 369:1561-1563.
6. Behin A, Hoang-Xuan K, Carpentier AF, Delattre JY (2003) Primary brain tumours in adults. Lancet 361:323-331.
7. Hamilton GS (2015) Antibody-drug conjugates for cancer therapy: The technological and regulatory challenges of developing drug-biologic hybrids. Biologicals 43:318-332. doi: 10.1016/j.biologicals.2015.05.006
8. de Goeij BE, Lambert JM (2016) New developments for antibody-drug conjugate-based therapeutic approaches. Curr Opin Immunol 40:14-23.
9. Ledford H (2016) Weaponized antibodies use new tricks to fight cancer. Nature 540:19-20.
10. Reardon DA, Lassman AB, van den Bent M, Kumthekar P, Merrell R, Scott AM, Fichtel L, Sulman EP, Gomez E, Fischer J, Lee HJ, Munasinghe W, Xiong H, Mandich H, Roberts-Rapp L, Ansell P, Holen KD, Gan HK (2016) Efficacy and safety results of

555 ABT-414 in combination with radiation and temozolomide in newly diagnosed
556 glioblastoma. Neuro Oncol doi: 10.1093/neuonc/now257
557 11. Fermani S, Falini G, Ripamonti A, Bolognesi A, Polito L, Stirpe F (2003) Crystallization
558 and preliminary X-ray diffraction analysis of two ribosome-inactivating proteins: lychnin
559 and dianthin 30. Acta Crystallogr D Biol Crystallogr 59:1227-1229.
560 12. Hosur MV, Nair B, Satyamurthy P, Misquith S, Surolia A, Kannan KK (1995) X-ray
561 structure of gelonin at 1.8 A resolution. J Mol Biol 250:368-80.
562 13. von Mallinckrodt B, Thakur M, Weng A, Gilabert-Oriol R, Durkop H, Brenner W, Lukas
563 M, Beindorff N, Melzig MF, Fuchs H (2014) Dianthin-EGF is an effective tumor
564 targeted toxin in combination with saponins in a xenograft model for colon carcinoma.
565 Future Oncol 10:2161-2175.
566 14. Thakur M, Mergel K, Weng A, von Mallinckrodt B, Gilabert-Oriol R, Durkop H, Melzig
567 MF, Fuchs H (2013) Targeted tumor therapy by epidermal growth factor appended
568 toxin and purified saponin: an evaluation of toxicity and therapeutic potential in
569 syngeneic tumor bearing mice. Mol Oncol 7:475-483.
570 15. Weng A, Manunta MD, Thakur M, Gilabert-Oriol R, Tagalakis AD, Eddaoudi A, Munye
571 MM, Vink CA, Wiesner B, Eichhorst J, Melzig MF, Hart SL (2015) Improved
572 intracellular delivery of peptide- and lipid-nanoplexes by natural glycosides. J Control
573 Release 206:75-90. doi: 10.1016/j.jconrel.2015.03.007
574 16. Furness SG, Liang YL, Nowell CJ, Halls ML, Wookey PJ, Dal Maso E, Inoue A,
575 Christopoulos A, Wootten D, Sexton PM (2016) Ligand-Dependent Modulation of G
576 Protein Conformation Alters Drug Efficacy. Cell 167:739-749.e11. doi:
577 10.1016/j.cell.2016.09.021
578 17. Wookey P, Zulli A, Lo C, Hare D, Schwarer A, Darby I, Leung A (2010) Calcitonin
579 receptor (CTR) expression in embryonic, foetal and adult tissues: developmental and
580 pathophysiological implications. In: Hay D, Dickerson I (eds) The calcitonin gene-

related peptide family; form, function and future perspectives. Springer, Netherlands. pp199-233.

18. Wookey PJ, Turner K, Furness JB (2012) Transient expression of the calcitonin receptor by enteric neurons of the embryonic and early post-natal mouse. Cell Tissue Res 347:311-317.
19. Marx SJ, Aurbach GD, Gavin JR, 3rd, Buell DW (1974) Calcitonin receptors on cultured human lymphocytes. J Biol Chem 249:6812-6816.
20. Body JJ, Glibert F, Nejai S, Fernandez G, Van Langendonck A, Borkowski A (1990) Calcitonin receptors on circulating normal human lymphocytes. J Clin Endocrinol Metab 71:675-681.
21. Jagger C, Chambers T, Pondel M (2000) Transgenic mice reveal novel sites of calcitonin receptor gene expression during development. Biochem Biophys Res Commun 274:124-129.
22. Tikellis C, Xuereb L, Casley D, Brasier G, Cooper ME, Wookey PJ (2003) Calcitonin receptor isoforms expressed in the developing rat kidney. Kid Int 63:416-426.
23. Tolcos M, Tikellis C, Rees S, Cooper M, Wookey P (2003) Ontogeny of calcitonin receptor mRNA and protein in the developing central nervous system of the rat. J Comp Neurol 456: 29-38.
24. Furness SGB, Hare DL, Kourakis A, Turnley AM, Wookey PJ (2016) A novel ligand of calcitonin receptor reveals a potential new sensor that modulates programmed cell death. Cell Death Discov 2:16062. eCollection 2016. doi: 10.1038/cddiscovery.2016.62
25. Wookey PJ, McLean CA, Hwang P, Furness SG, Nguyen S, Kourakis A, Hare DL, Rosenfeld JV (2012) The expression of calcitonin receptor detected in malignant cells of the brain tumour glioblastoma multiforme and functional properties in the cell line A172. Histopathology 60:895-910. doi: 10.1111/j.1365-2559.2011.04146.x

26. Silvestris F, Cafforio P, De Matteo M, Quatraro C, Dammacco F (2008) Expression and function of the calcitonin receptor by myeloma cells in their osteoclast-like activity in vitro. Leuk Res. 32:611-623.
27. Venkatanarayan A, Raulji P, Norton W, Chakravarti D, Coarfa C, Su X, Sandur SK, Ramirez MS, Lee J, Kingsley CV, Sananikone EF, Rajapakshe K, Naff K, Parker-Thornburg J, Bankson JA, Tsai KY, Gunaratne PH, Flores ER (2015) IAPP-driven metabolic reprogramming induces regression of p53-deficient tumours in vivo. Nature. 517:626-630.
28. Nicholson GC, Horton MA, Sexton PM, D'Santos CS, Moseley JM, Kemp BE, Pringle JA, Martin TJ (1987) Calcitonin receptors of human osteoclastoma. Horm Metab Res. 19:585-589.
29. Gorn AH, Rudolph SM, Flannery MR, Morton CC, Weremowicz S, Wang TZ, Krane SM, Goldring SR (1995) Expression of two human skeletal calcitonin receptor isoforms cloned from a giant cell tumor of bone. The first intracellular domain modulates ligand binding and signal transduction. J Clin Invest. 95:2680-2691.
30. Gillespie M, Thomas R, Pu Z, Zhou H, Martin T, Findlay D (1997) Calcitonin receptors, bone sialoprotein and osteopontin are expressed in primary breast cancers. Int J Cancer. 73:812-815.
31. Wu G, Burzon D, di Sant'Agnese P, Schoen S, Deftos L, Gershagen S, Cockett A (1996) Calcitonin receptor mRNA expression in human prostate. Urol. 47:376-381.
32. Thomas S, Muralidharan A, Shah GV (2007) Knock-down of calcitonin receptor expression induces apoptosis and growth arrest of prostate cancer cells. Int J Oncol. 31:1425-1437.
33. Frendo JL, Delage-Mourroux R, Cohen R, Pichaud F, Pidoux E, Guliana JM, Jullienne A (1998) Calcitonin receptor mRNA is expressed in human medullary thyroid carcinoma. Thyroid 8:141-147.

633 34. Scott AM, Wolchok JD, Old LJ (2012) Antibody therapy of cancer. Nat Rev Cancer. 12:
634 278-287.
635 35. Verhaak RG, Hoadley KA, Purdom E, Wang V, Qi Y, Wilkerson MD, Miller CR, Ding L,
636 Golub T, Mesirov JP, Alexe G, Lawrence M, O'Kelly M, Tamayo P, Weir BA, Gabriel S,
637 Winckler W, Gupta S, Jakkula L, Feiler HS, Hodgson JG, James CD, Sarkaria JN,
638 Brennan C, Kahn A, Spellman PT, Wilson RK, Speed TP, Gray JW, Meyerson M, Getz
639 G, Perou CM, Hayes DN, Cancer Genome Atlas Research, Network (2010) Integrated
640 genomic analysis identifies clinically relevant subtypes of glioblastoma characterized
641 by abnormalities in PDGFRA, IDH1, EGFR, and NF1. Cancer Cell 17:98-110.
642 36. Day BW, Stringer BW, Al-Ejeh F, Ting MJ, Wilson J, Ensbey KS, Jamieson PR, Bruce
643 ZC, Lim YC, Offenhauser C, Charmsaz S, Cooper LT, Ellacott JK, Harding A, Leveque
644 L, Inglis P, Allan S, Walker DG, Lackmann M, Osborne G, Khanna KK, Reynolds BA,
645 Lickliter JD, Boyd AW (2013) EphA3 maintains tumorigenicity and is a therapeutic
646 target in glioblastoma multiforme. Cancer Cell 23:238-248.
647 37. Pollard SM, Yoshikawa K, Clarke ID, Danovi D, Stricker S, Russell R, Bayani J, Head
648 R, Lee M, Bernstein M, Squire JA, Smith A, Dirks P (2009) Glioma stem cell lines
649 expanded in adherent culture have tumor-specific phenotypes and are suitable for
650 chemical and genetic screens. Cell Stem Cell 4:568-580.
651 38. Francisco JA, Cerveny CG, Meyer DL, Mixan BJ, Klussman K, Chace DF, Rejniak SX,
652 Gordon KA, DeBlanc R, Toki BE Law CL, Doronina SO, Siegall CB Senter PD, Wahl
653 AF (2003) cAC10-vcMMAE, an anti-CD30-monomethyl auristatin E conjugate with
654 potent and selective antitumor activity. Blood 102:1458-65.
655 39. Grundy TJ, De Leon E, Griffin KR, Stringer BW, Day BW, Fabry B, Cooper-White J,
656 O'Neill GM (2016) Differential response of patient-derived primary glioblastoma cells to
657 environmental stiffness. Scientific Reps 6: 23353.

40. Tivnan A, Zhao J, Johns TG, Day BW, Stringer BW, Boyd AW, Tiwari S, Giles KM, Teo C, McDonald KL (2014) The tumor suppressor microRNA, miR-124a, is regulated by epigenetic silencing and by the transcriptional factor, REST in glioblastoma. Tumour Biol 35:1459-1465.
41. Hosein AN, Lim YC, Day B, Stringer B, Rose S, Head R, Cosgrove L, Sminia P, Fay M, Martin JH (2015) The effect of valproic acid in combination with irradiation and temozolomide on primary human glioblastoma cells. J Neuro-oncol 122:263-271.
42. Dickinson A, Yeung KY, Donoghue J, Baker MJ, Kelly RD, McKenzie M, Johns TG, St John JC (2013) The regulation of mitochondrial DNA copy number in glioblastoma cells. Cell Death Differ 20:1644-1653.
43. Gilabert-Oriol R, Weng A, Trautner A, Weise C, Schmid D, Bhargava C, Niesler, N. Wookey PJ, Fuchs H, Thakur M (2015) Combinatorial approach to increase efficacy of Cetuximab, Panitumumab and Trastuzumab by dianthin conjugation and co-application of SO1861. Biochem Pharmacol 97:247-255.
44. Rosenblum MG, Kohr WA, Beattie KL, Beattie WG, Marks W, Toman PD, Cheung L (1995) Amino acid sequence analysis, gene construction, cloning, and expression of gelonin, a toxin derived from Gelonium multiflorum. J Interfer Cyto Res 15: 547-555.
45. Cumber AJ, Henry RV, Parnell GD, Wawrzynczak EJ (1990) Purification of immunotoxins containing the ribosome-inactivating proteins gelonin and momordin using high performance liquid immunoaffinity chromatography compared with blue sepharose CL-6B affinity chromatography. J Immunol Methods 135:15-24.
46. Weng A, Thakur M, von Mallinckrodt B, Beceren-Braun F, Gilabert-Oriol R, Wiesner B, Eichhorst J, Böttger S, Melzig MF, Fuch H (2012) Saponins modulate the intracellular trafficking of protein toxins. J Control Release 164:74-86. doi: 10.1016/j.jconrel.2012.10.002

683 47. Seck T, Baron R, Horne WC (2003) Binding of filamin to the C-terminal tail of the
684 calcitonin receptor controls recycling. J Biol Chem 278:10408-10416.
685 48. Ross JL, Ali MY, Warshaw DM (2008) Cargo transport: molecular motors navigate a
686 complex cytoskeleton. Curr Op Cell Biol 20:41-47.
687 49. Cizeau J, Grenkow DM, Brown JG, Entwistle J, MacDonald GC (2009) Engineering
688 and biological characterization of VB6-845, an anti-EpCAM immunotoxin containing a
689 T-cell epitope-depleted variant of the plant toxin bouganin. J Immunother 32:574-84.
690
691
692 **Figure legends**
693 **Figure 1**
694 Expression of CTR on different cell lines, gel electrophoresis of samples taken during
695 conjugation of mAb2C4 to dianthin-30[His^6] and final products for the syntheses of
696 mAb2C4:dianthin-30[His^6], mAb2C4:gelonin and mAb2C4:MMAE.
697 (a) Immunoblot of whole cell lysates prepared from SB2b (lane 1), PB1 (lane 2), U87MG
698 (lane 3) WK1 (lane 4) and JK2 (lane 5) stained with mAb1H10 anti-human CTR antibody
699 and U87 stained with mAb2C4 (lane 6); U87MG stained with anti-β-tubulin antibody (lane
700 7). It is likely that band ‘b’ represents the full length hCTR protein without glycosylation and
701 band ‘a’ the N-terminal truncated form with the absence of epitope 4 to which mAb2C4
702 binds. Band ‘c’ represents the extracellular domain (~14 kD) cleaved from the 40 kD
703 protein.
704 (b) Samples were assayed following the conjugation reaction (the molar ratio of
705 proteins:crosslinker SPDP was 1:6 and the molar ratio of activated dianthin-30[His^6] and
706 mAb2C4 was 1:1). The sample was non-reduced (lane 1) or reduced (lane 2) and for
707 controls, mAb2C4 was non-reduced (lane 3) or reduced (lane 4). The mAb2C4:dianthin-
708 30[His^6] conjugates are indicated with an arrowhead and dianthin-30 with arrows.

(c) Purified mAb2C4:dianthin-30[His^6] (lane 1) compared to mAb2C4 (lane 2) and dianthin-30[His^6] (lane 3).

(d) Purified mAb2C4:gelonin (lane 1) compared to gelonin (lane 2) and mAb2C4 (lane 3).

(e) Purified mAb2C4:MMAE (lane 1) compared to mAb2C4 (lane 2).

Figure 2

(a) The comparative toxicity profiles of the immunotoxin mAb2C4:dianthin-30 with (●, 3 µg/mL, n=4) and without (■) SO1861 (n=4), and (b) the ADC, mAb2C4:MMAE with (●, n=3) and without (■, n=4) SO1861 in the HGG cell line SB2b. (c) The comparative toxicity profiles of the immunotoxin mAb2C4:dianthin-30 (■, n=3) and the ADC, mAb2C4:MMAE (●, n=3) in the cell line U87MG with 1 µg/mL SO1861. In any one 96-well experiment to measure lactate dehydrogenase (LDH) activity, each data point represents the nett LDH activity in which the nett LDH is calculated from the difference between the mean total LDH (3 lysed cell samples) minus mean residual LDH (3 un-lysed cell samples). Each experiment was repeated n=3 or n=4 as indicated above. Values were normalised against the mean of LDH activity in untreated cells that results in % maximal LDH activity. The EC_{50} values are listed in Table 1.

Figure 3

Typical uptake of mAb2C4:AF568 (red) by HGG cell lines and intracellular localisation in relation to the distribution of LAMP1-positive (green) lysosomes within the cytoplasmic domain and to nuclei stained with DAPI (blue).

(a) Merged image following the uptake of mAb2C4:AF568 (red) by cell line JK2.

(b) Merged image following the uptake of mAb2C4:AF568 by the cell lines SB2b.

(c) Image of PB1 (red channel).

735 (d) Merged image of PB1.

736 (e) Image of U87MG (red channel).

737 (f) Merged image of U87MG.

738 A subset of fluorescence in the red channel coincides with LAMP1 staining (green in the
739 merged images in panels e & f) as shown in yellow [overlap]. The calibration bar in (f)
740 represents 40 µm in (a), 6 µm in (b) and 10 µm in (c-f).

741

742 **Figure 4**

743 Intracellular localisation of dianthin:AF488 and release into the cytosol in the presence of
744 SO1861.

745 (a) U87MG cells were stained with the membrane permeable dye Hoechst 33342 (blue
746 nuclei),

747 (b) pHrodo™ Red Dextran (red),

748 (c) dianthin:AF488 (green) and

749 (d) merged image. Co-localization with pHrodo™ Red Dextran and dianthin-30:AF488 was
750 partly observed (white arrows), indicating accumulation in endosomes/lysosomes.

751 (e) shows the increase in the fluorescence intensity with the release of dianthin:AF488 into
752 the cytosol in cell 1 (green trace) and cell 2 (blue trace). Regions of interest were defined
753 for affected cells and the SO1861 mediated intracellular release of dianthin:AF488 was
754 analysed off-line by Carl Zeiss ZEN 2.3 lite software. The sudden increase of the intensity
755 indicates the release of dianthin:AF488 into the cytosol.

756 (f-i) images taken from the supplementary video, show the time series of SO1861
757 mediated intracellular release of dianthin:AF488 from two cells in a field, in which merged
758 images at different time points are shown, of U87MG cells loaded with dianthin:AF488.

759 (f) t=36 s, 5 µg/mL SO1861 was added.

760 (g) t= 136 s, no change.

(h) t=180 s, high intensity green fluorescence is evident in cell 1, which indicates the SO1861 mediated intracellular release of dianthin:AF488 into the cytosol. At 500 s, the leakage of dianthin:AF488 into the supernatant was restricted by the plasma membrane and is approximately 25% over 5 minutes (green trace).

(i) t=504 s, high intensity green fluorescence is evident in cell 2, which indicates the SO1861 mediated intracellular release of dianthin:AF488 into the cytosol.

The calibration bar in (a) represents 20 µm.

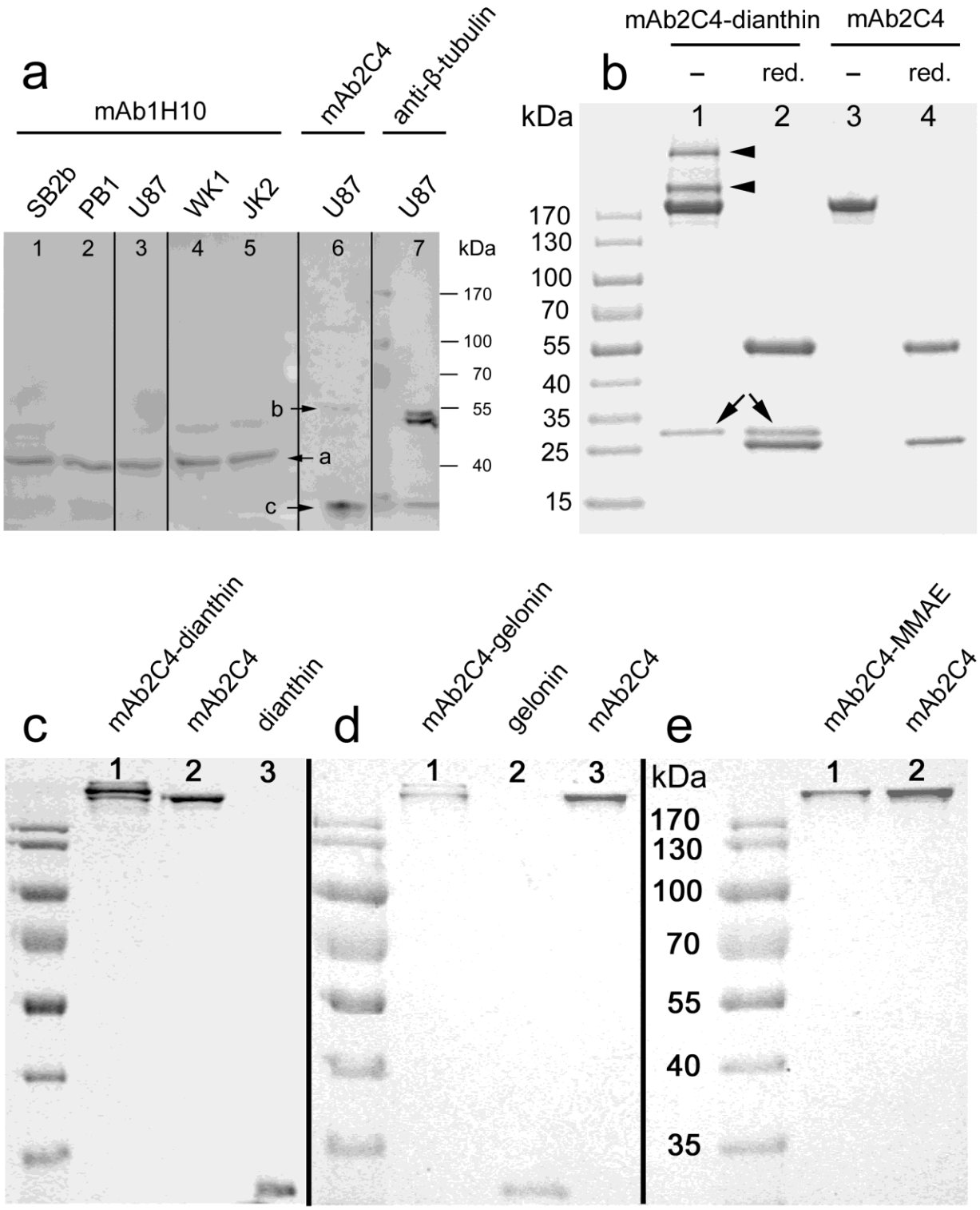
a
mAb1H10
mAb2C4
anti-β-tubulin
SB2b
PB1
U87
WK1
JK2
U87
U87
1 2 3 4 5 6 7
kDa
170
100
70
55
40
b
c
b
mAb2C4-dianthin
mAb2C4
–
red.
–
red.
kDa
1 2 3 4
170
130
100
70
55
40
35
25
15
c
mAb2C4-dianthin
mAb2C4
dianthin
1 2 3
d
mAb2C4-gelonin
gelonin
mAb2C4
1 2 3
e
mAb2C4-MMAE
mAb2C4
kDa
1 2
170
130
100
70
55
40
35

768

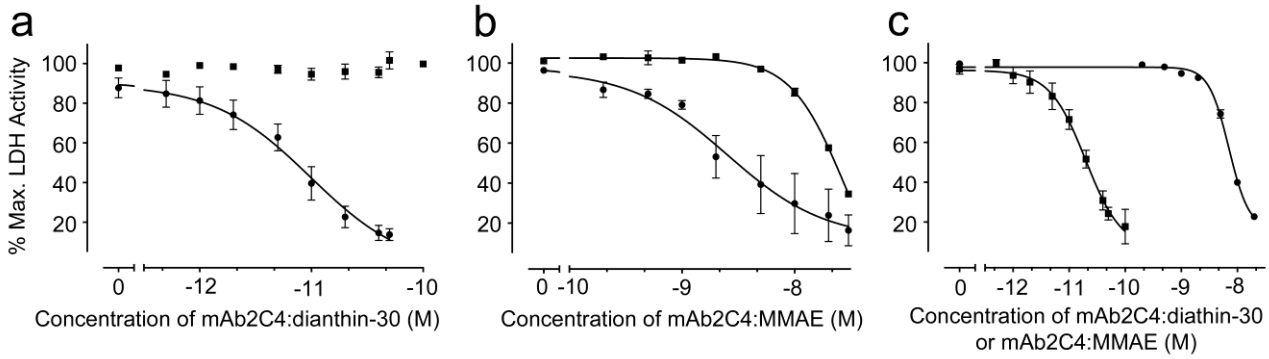
a
b
c
% Max. LDH Activity
100
80
60
40
20
0
-12
-11
-10
-9
-8
Concentration of mAb2C4:dianthin-30 (M)
Concentration of mAb2C4:MMAE (M)
Concentration of mAb2C4:diathin-30
or mAb2C4:MMAE (M)

769

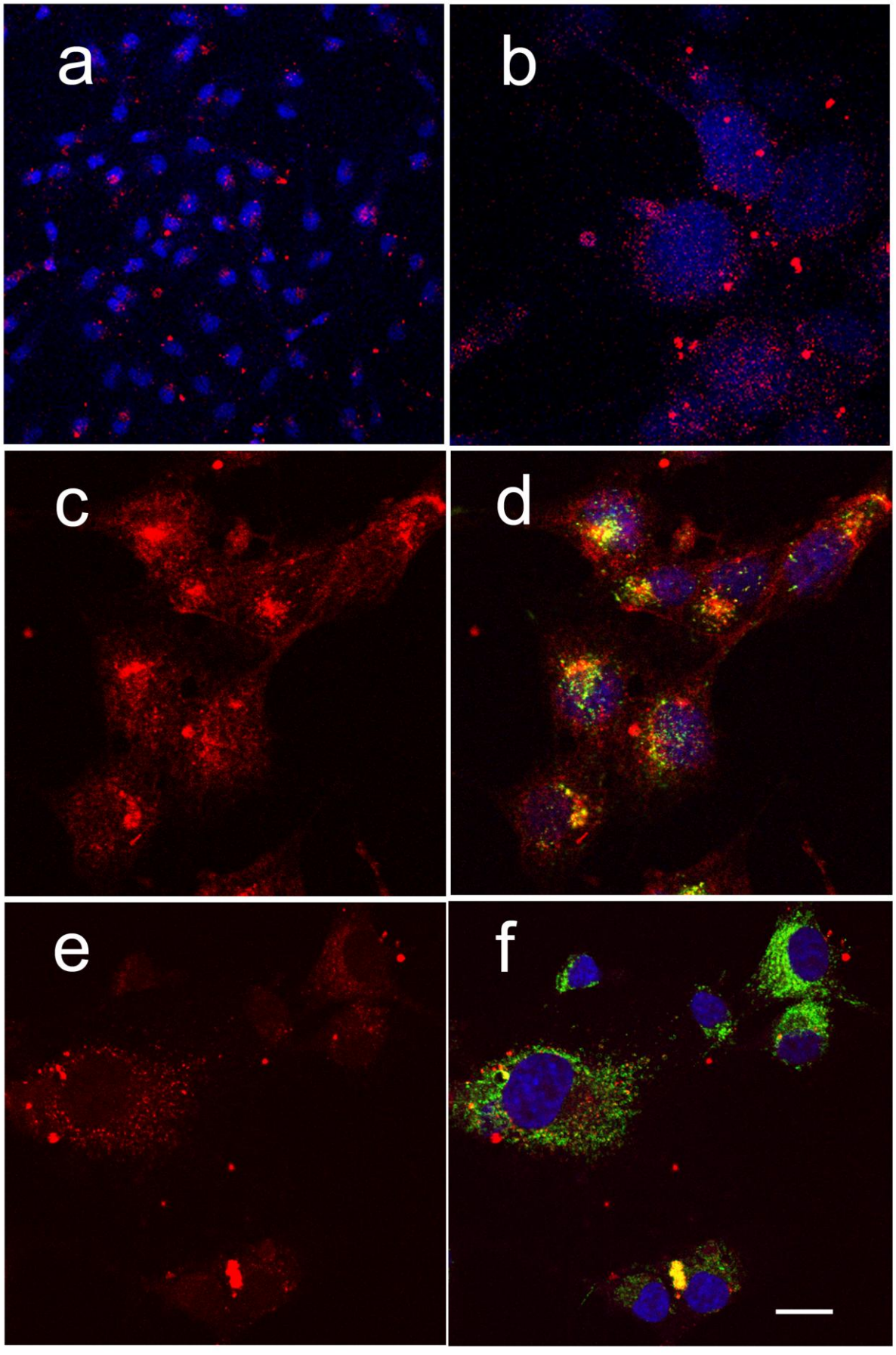

770

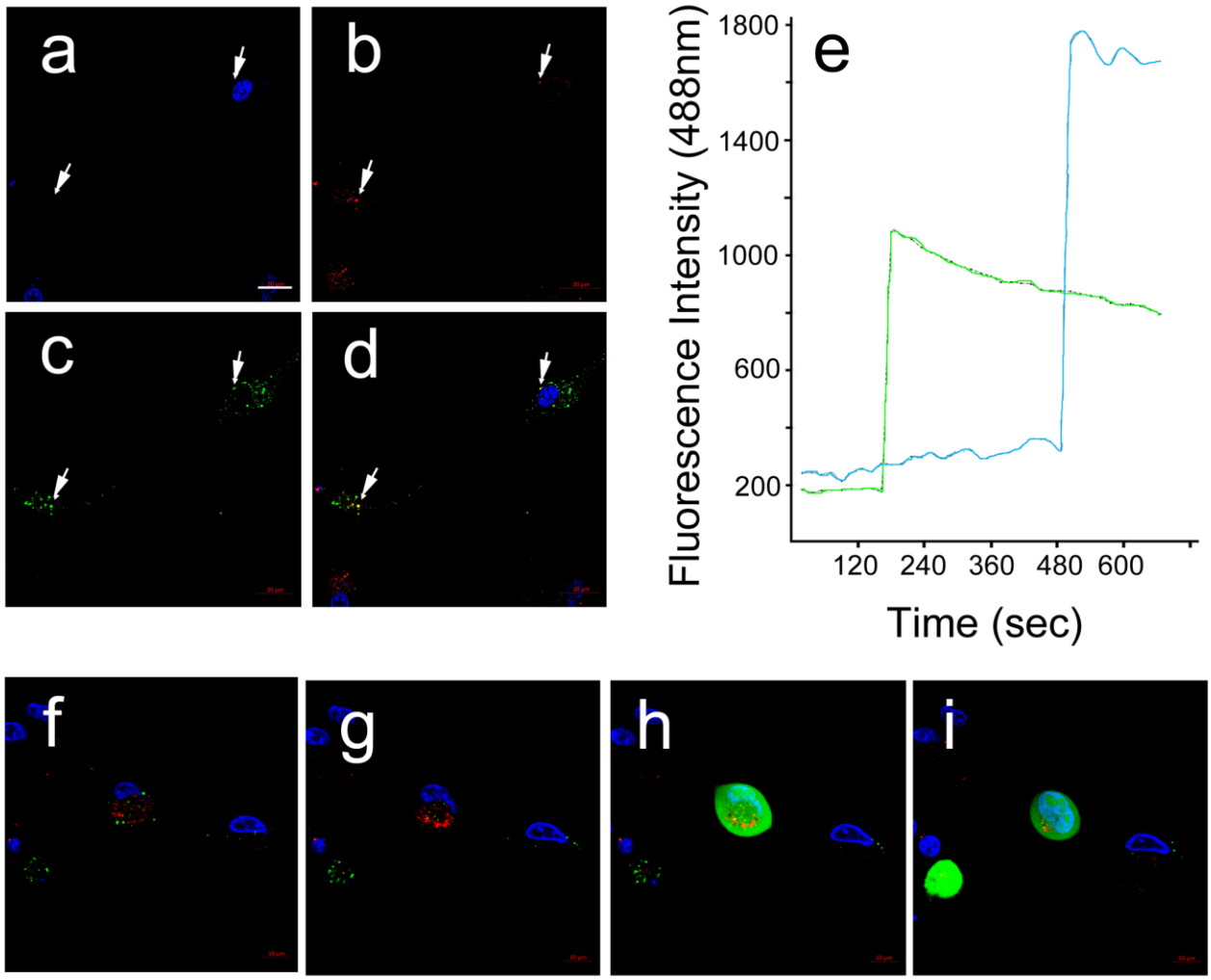

771

772 **Table 1:** EC_{50} values derived from Fig. 2 are listed with different cell lines using
773 immunotoxins mAb2C4:dianthin-30[His^6], mAb2C4:gelonin, and the ADC mAb2C4:MMAE
774 in the LDH release assay as described for Fig. 2. Each determination represents data from
775 n independent experiments. Also included are data derived from supplementary figure 4.
776 ND = No curve could be determined from data over the tested range 1-100pM. ND* the
777 EC_{50} could be estimated from supplementary figure 6 as approximately 10-20 nM.

778
779
780
781

Cell line	Immunotoxin/ADC	Addition of SO1861	Independent experiments (n)	Log EC_{50}	EC_{50}
SB2b	mAb2C4:dianthin	nil	4	ND	ND*
	mAb 2C4:dianthin	3 µg/mL	4	-11.0±0.14	10.0 pM
	mAb 2C4:MMAE	nil	4	-7.6±0.23	25.1 nM
	mAb 2C4:MMAE	3 µg/mL	3	-8.6±0.20	2.5 nM
U87MG	mAb 2C4:dianthin	1 µg/mL	3	-10.7±0.11	20.0 pM
	mAb 2C4:MMAE	1 µg/mL	3	-8.2±0.02	6.3 nM
	mAb 2C4:gelonin	1 µg/mL	3	-10.7±0.1	20 pM
JK2	mAb 2C4:dianthin	3 µg/mL	4	-11.0±0.33	10.0 pM

Author/s:
Gilabert-Oriol, R; Furness, SGB; Stringer, BW; Weng, A; Fuchs, H; Day, BW; Kourakis, A; Boyd, AW; Hare, DL; Thakur, M; Johns, TG; Wookey, PJ

Title:
Dianthin-30 or gelonin versus monomethyl auristatin E, each configured with an anti-calcitonin receptor antibody, are differentially potent in vitro in high-grade glioma cell lines derived from glioblastoma

Date:
2017-09-01

Citation:
Gilabert-Oriol, R., Furness, S. G. B., Stringer, B. W., Weng, A., Fuchs, H., Day, B. W., Kourakis, A., Boyd, A. W., Hare, D. L., Thakur, M., Johns, T. G. & Wookey, P. J. (2017). Dianthin-30 or gelonin versus monomethyl auristatin E, each configured with an anti-calcitonin receptor antibody, are differentially potent in vitro in high-grade glioma cell lines derived from glioblastoma. CANCER IMMUNOLOGY IMMUNOTHERAPY, 66 (9), pp.1217-1228. https://doi.org/10.1007/s00262-017-2013-z.